Al-Hikmah Journal of Pure and Applied Sciences
©2026
Volume 9 Issue 1: 33-44

Characterization and Application of Chicken Feather Activated Carbon for the Removal of Rhodamine B from Aqueous Solution

*Subair, M.K. and Adekola, F.A.

Department of Industrial Chemistry, Faculty of Physical Sciences, University of Ilorin, Ilorin, Nigeria.

ARTICLE INFO

Article history

Received: 01/12/2025
Revised: 20/03/2026
Accepted: 23/04/2026
Published: 08/05/2026

Doi:
https://doi.org/10.5281/zenodo.20072946

Keywords:

Chicken Feather,
Activated Carbon,
Rhodamine B,
Adsorption
Phosphoric acid

Corresponding Author

Email:
subair.mk1@unilorin.edu.ng

Phone: +234818 529 8441

ABSTRACT

Chicken feather derived activated carbon (CFAC) was prepared via chemical activation using H_3PO_4 and evaluated for the removal of Rhodamine B (RhB) from aqueous solutions. The adsorbent was characterized using Fourier transform infrared spectroscopy (FTIR), scanning electron microscopy (SEM), and Brunauer–Emmett–Teller (BET) analysis. CFAC exhibited a specific surface area of 48.140 m^2/g, a pore volume of 0.057 cm^3/g, and an average pore diameter of 2.647 nm. Batch adsorption experiments demonstrated efficient RhB removal, achieving an adsorption capacity of 99.28 mg/g and a removal efficiency of 98.42 % under optimal conditions (pH 6, contact time of 180 min, and temperature of 30 °C). The solution pH was adjusted using 0.1 M HCl or 0.1 M NaOH, and the effect of pH was investigated over a range of 2–12. The influences of solution pH, adsorbent dosage, and contact time on adsorption performance were systematically examined. Kinetic studies revealed that the adsorption process followed pseudo-first-order and Elovich models, while equilibrium data were best described by the Langmuir and Temkin isotherm models. Physicochemical properties, including bulk density, moisture content, ash content, iodine value, and conductivity, were also determined. The results indicate that TCFs-Pa is an effective and environmentally sustainable adsorbent with significant potential for the treatment of dye-contaminated wastewater.

Citation: Subair, M.K. and Adekola, F.A. (2026). Characterization and Application of Chicken Feather Activated Carbon for the Removal of Rhodamine B from Aqueous Solution. *AJPAS.* 9(1): 33-44

1.0 Introduction

The removal of harmful dyes like Rhodamine B from aqueous solutions is crucial for environmental protection and human health [21]. Adsorption is a widely used method for dye removal due to its low-cost, design and operational flexibility and efficiency; and activated carbon is a popular adsorbent due to its high surface area and adsorption capacity [16]. However, the high cost and limited availability of commercial activated carbons have led to the search for alternative, sustainable adsorbents [23]. Chicken feathers, a waste biomass, have been explored as a potential precursor for activated carbon production [9]. The use of phosphoric acid as an activating agent has been shown to enhance the surface properties and adsorption capacity of chicken feather-based activated carbon (CFAC) [16].

Generally, activated carbons (ACs) are prepared either by physical or chemical activation method where the latter is preferred owing to the simplicity, lower temperature, shorter activation time, higher yield, and good development of the porous structure [5]. This study investigates the preparation and application of CFAC, using phosphoric acid as an activating agent, for the removal of Rhodamine B from aqueous solutions. The surface properties and adsorption capacity of CFAC are evaluated, and the effects of pH, contact time, and initial dye concentration on Rhodamine B removal are examined [10].

2.0 Materials and Method

2.1 Adsorbent preparation

Chicken Feather was sourced from Ollan Farm at upper Gaa -Akanbi in Ilorin, Kwara State, Nigeria. It was double-washed with distilled water to remove dust and organic matter, then sun-dried for 10 hours. The Chicken Feathers was carbonized at 300°C for 30 minutes and dried in a desiccator. Thereafter, Phosphoric acid (H_3PO_4) treatment was done following the method reported by Zhang *et al*.,[28] with little modification: The 30 g carbonized material was soaked with 1.0 M Orthophosphoric acid in a beaker in mass ratio (Chicken Feathers to Phosphoric acid) of 1:2 and thus the activated carbon was achieved by filtration using Whatman Filter Paper No. 42 and washed with doubly deionized water to obtain neutral of pH 7. The activated carbon was thereafter dried in an oven at 105 ^oC for 2 hours. The resulting material, was then named TCFs-Pa, was stored in an airtight container for subsequent operations.

2.2 Characterization of Chicken feather activated with H_3PO_4 (TCFs-Pa)

Physico-chemical analysis of TCFs-Pa (Chicken feathers-derived activated carbon) was performed to its characteristic properties, including pH, bulk density, ash content, moisture content, iodine value, and conductivity. The results are presented in Table 1. Furthermore, advanced characterization techniques, namely Scanning Electron Microscopy/Energy-Dispersive X-ray Spectroscopy (SEM/EDX) and Fourier Transform Infrared spectroscopy (FTIR) and Brunauer–Emmett–Teller (BET), were employed to elucidate the surface morphology, elemental composition, and molecular structure of the activated carbon, providing a comprehensive understanding of its properties and potential applications [13].

2.3 Adsorption Experiment

The maximum absorption peak of RhB when a known concentration of its solution was scanned between 200 and 1000 nm. Maximum adsorption was obtained at 554 nm therefore the residual concentration after absorption was determined at λ_{max}. Correlation coefficient R^2 greater than 0.9943 shows the linearity of the calibration curve. UV/Visible Spectrophotometry was therefore adopted for the analysis of residual Rhodamine B in subsequent experiments. The adsorption of Rhodamine B (RhB) from aqueous solution onto chicken feathers activated with H_3PO_4 was investigated using batch experiments. Rhodamine B solutions with initial concentrations range of 1.0-10 mg L^{-1} were prepared and equilibrated with 0.1 g of TCFs-Pa in 250 mL conical flasks, then agitated at 150 rpm for 30-240 min at 30-70°C. The filtrate was analyzed by UV/Visible Spectrophotometer (Jenway 7300 spectrophotometer) [2], to determine the adsorption capacity. The quantity of RhB adsorbed

(qe) was calculated by equation (i) and the percentage removal was calculated using equation (ii), where Co and Ce are the initial and final concentrations, m is the adsorbent dosage, and V is the volume of solution (mL) [24].

$$q_e = \left(\frac{C_o - C_e}{m}\right) V \quad \text{(i)}$$

$$\text{Removal (\%)} = \left(\frac{C_o - C_e}{C_o}\right) X100 \quad \text{(ii)}$$

3.0 Results and Discussion

The results presented in Table 1 provide a comprehensive overview of the physical and chemical properties of TCFs-Pa, including its pH, bulk density, ash content, moisture content, iodine number, and conductivity, which are essential for evaluating its suitability for various industrial applications. The discrepancy observed between the original and revised iodine values may be attributed to variations in experimental conditions, including differences in titration methodology and endpoint determination, sample preparation procedures such as drying conditions and particle sized istribution. The iodine number (mg g^{-1}) is widely used as an indirect indicator of micropore volume and microporous surface area in activated carbons. The relatively low BET surface area of CFAC (48.140 m^2 g^{-1}) is consistent with a moderate iodine value, suggesting limited development of microporosity. In contrast, activated carbons with well-developed microporous structures and higher BET surface areas are generally exhibit higher iodine numbers

Table 1 Proximate analysis of TCFs-Pa

Parameter	Value
pH	7.9
Bulk Density (g/cm^3)	0.99
Moisture Content (%)	0.4
Ash Content (%)	3.0
Iodine Number (mg/g)	≈ 550
Conductivity (µSm)	0.31

3.1 FTIR SPECTRA of TCFs-PA before and after adsorption of Rhodamine B

The FTIR spectra of TCFs-PA before and after adsorption reveal significant changes, indicating successful adsorption figure 1. Key shifts include: O-H stretching (3429.778-3275.983cm^{-1}, minimal shift), C-H stretching (2938.501-2929.823 cm^{-1}), C=C stretching (1657.035-1651.732 cm^{-1},), and C=C bending (1489.1482.509cm-1). The shifts suggest alterations in alkyl group conformations, carbonyl group bonding, and aromatic ring conformations, while O-H and C-O stretching vibrations remain relatively unaffected. These changes provide valuable insights into the adsorption mechanism and molecular interactions between TCFs-PA and rhodamine B, indicating a complex adsorption process involving multiple functional groups.

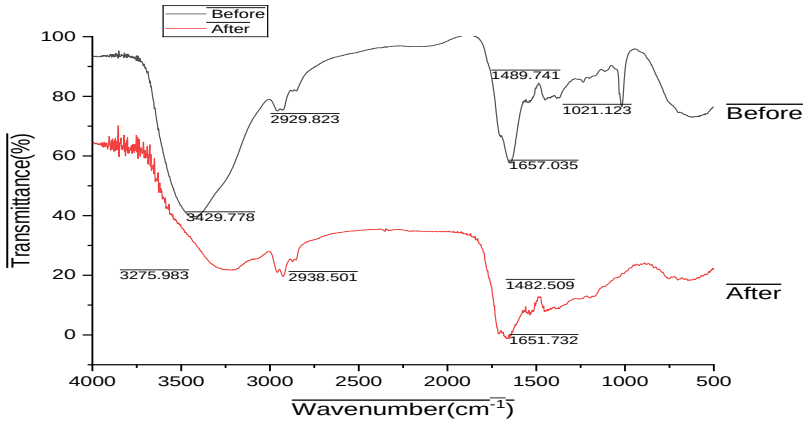

Fig. 1: The FTIR spectrum of TCFS-PA after adsorption of Rhodamine B

3.2 SEM/EDX Analysis for TCFs-Pa

The SEM/EDX analysis of TCFs-PA (Figure 2) confirmed the successful preparation of CFs-AC nanocomposite, revealing a major elemental composition of Oxygen (20.40%), Carbon (56.15%), Silicon (15.60%), Iron (3.42%), Potassium (1.21%), and Aluminum (3.22%). The presence of Si and Al detected in the BET/elemental analysis of chicken feather activated carbon (CFAC) has direct implications for Rhodamine B (RhB) adsorption. These elements may originate from the chemical activation process (e.g., H_3PO_4, reagents, or glassware) or be inherently present in the feather precursor as trace biological elements. Rhodamine B is a cationic dye, and the incorporation of Si- and Al-containing species introduces hydroxylated surface groups (Si–OH and Al–OH) that can deprotonate at pH values above the point of zero charge (pHpzc), generating negatively charged sites that enhance RhB uptake through electrostatic attraction. Additional adsorption contributions arise from hydrogen bonding between surface hydroxyl groups and RhB functional moieties, as well as π–π interactions between the aromatic structure of RhB and the carbonaceous framework of CFAC. However, excessive inorganic content may partially block pores or reduce available carbon active sites, potentially influencing adsorption capacity. The predominance of monolayer adsorption suggested by the Langmuir isotherm indicates that surface functional groups, rather than multilayer physical adsorption, play a dominant role in RhB uptake. Since the pHpzc of CFAC was not measured, the precise contribution of surface charge controlled electrostatic interactions cannot be conclusively established, representing a limitation of this study [11,15, 26].

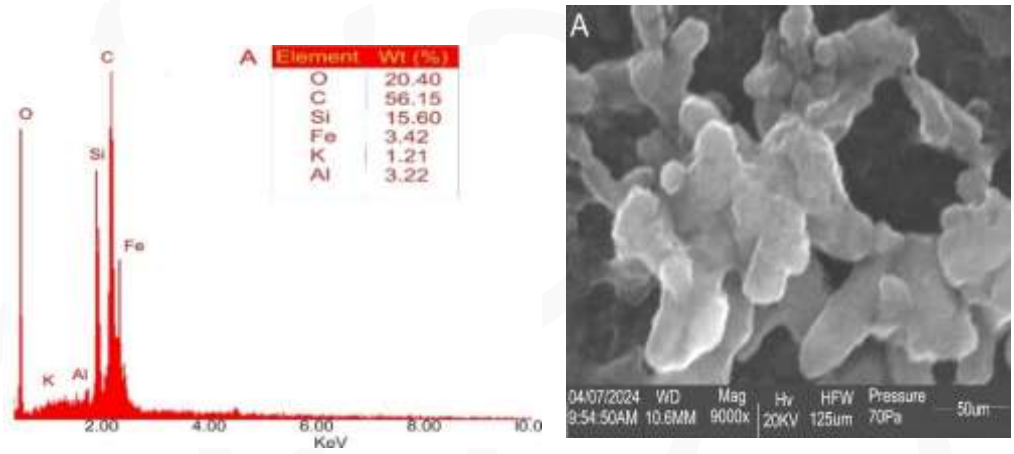

Fig. 2: SEM/EDX image of TCFs-PA before adsorption onto RhB

3.3 Effect of Initial Concentration of TCFs-Pa onto RhB

The adsorption capacity of TCFs-Pa for RhB dye decreased significantly from 98.8 mg/g to 91.7 mg/g as the initial concentration increased from 1 to 10 mg L^{-1}, aligning with previous reports of adsorbent surface saturation and reduced removal effectiveness at higher dye concentrations [8;18]. This decrease is primarily attributed to two factors: the increased number of RhB molecules competing for the limited adsorption sites on the TCFs-Pa surface, and the reduced diffusion rates of dye molecules from the bulk solution to the adsorbent surface [28]. This phenomenon is further supported by [23], highlighting the critical importance of optimizing initial dye concentrations to achieve efficient adsorption. Effective adsorption is contingent upon striking a balance between dye concentration and adsorbent capacity.

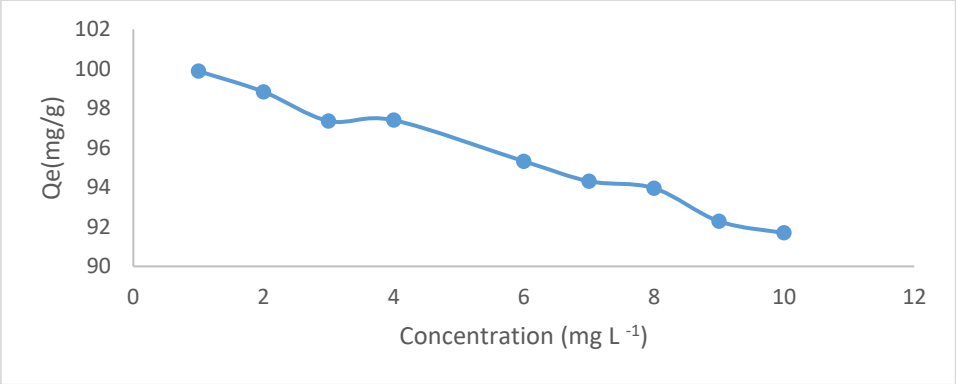

Fig 3 (a): Effect of Initial Concentration of TCFs-Pa onto RhB

3.4 Effect of Contact Time

The effect of contact time on Rhodamine B adsorption onto TCFs-Pa was examined, showing increased adsorption capacity up to 240 minutes, where equilibrium was established (Fig. 3b). Adsorption capacity rose slightly and gradually from 30 to 240 minutes, reaching 98.63 mg/g, due to available adsorption sites and facilitated electrostatic interactions. However, further increases beyond 240 minutes resulted in decreased adsorption capacity, indicating site saturation and reduced efficiency [12], highlighting the need for optimized contact time to achieve maximum adsorption capacity.

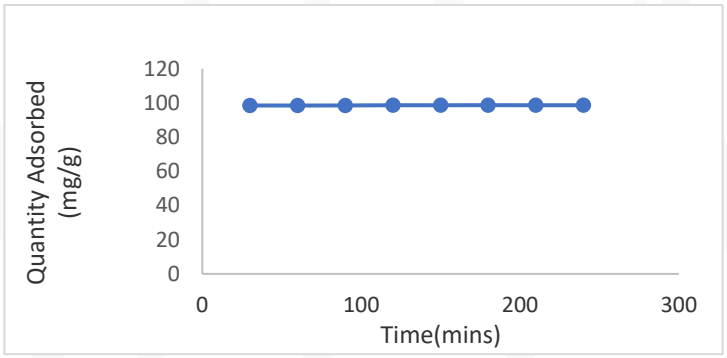

Fig. 3b: Effect of Contact Time on the adsorption of RhB onto TCFs-Pa

3.5 Effect of pH of TCFs-Pa onto RhB

The pH of the solution greatly influences adsorption process it determines the surface charge of the adsorbent and the state of adsorbate in solution. pH effects on the uptake of RhB onto TCFs-Pa were investigated and the highest adsorbed capacity uptake obtained at pH 6 was 99.3 mg/g. adsorbent dose (0.1 g/L), agitation speed (150 rpm), temperature (30 ^{o}C) and agitation time (180 mins)]

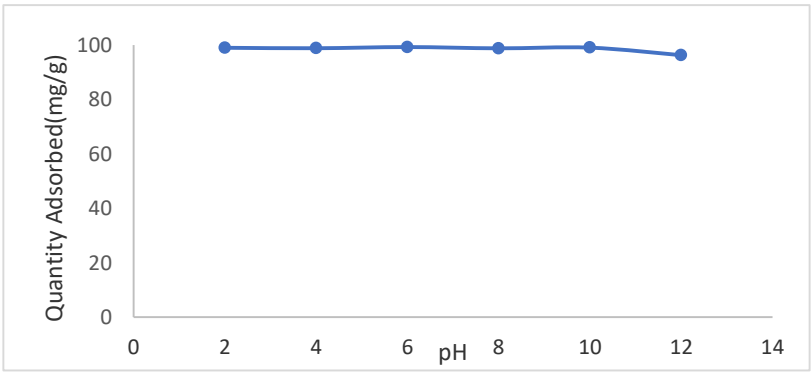

Fig. 3c: Effect of pH on the adsorption of RhB onto TCFs-Pa

3.6 Effect of Temperature of TCFs-Pa onto RhB

Figure 3d shows RhB adsorption onto TCFs-Pa peaked at 99.24 mg/g at 30°C, then decreased gradually to 96.51 mg/g at 70°C. Initially, elevated temperatures enhanced adsorption by reducing viscous forces, accelerating diffusion, and boosting kinetic energy [19]. However, beyond 30°C, increased thermal energy disrupted adsorbent-adsorbate interactions and enhanced molecular motion, potentially causing desorption and decreased adsorption capacity.

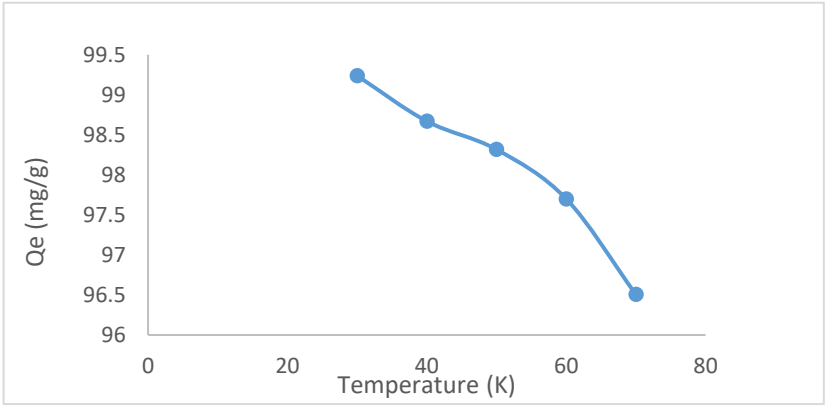

Fig. 3d: Effect of Temperature on the adsorption of RhB onto TCFs-Pa

3.7 Effect of Adsorbent Dosage onto TCFs-Pa

It could be observed that increase in adsorbent dosage resulted to decrease in adsorption capacity. This could be attributed to the aggregation or overlapping of the various adsorption sites thereby causing a decrease in total surface area and subsequently lower the adsorption capacity. A similar observation has been reported in literature by Shirvanimoghaddam *et al*., [20]. The maximum adsorption capacity achieved was 99.1 mg/g using optimum adsorbent dosage of 0.3 g.

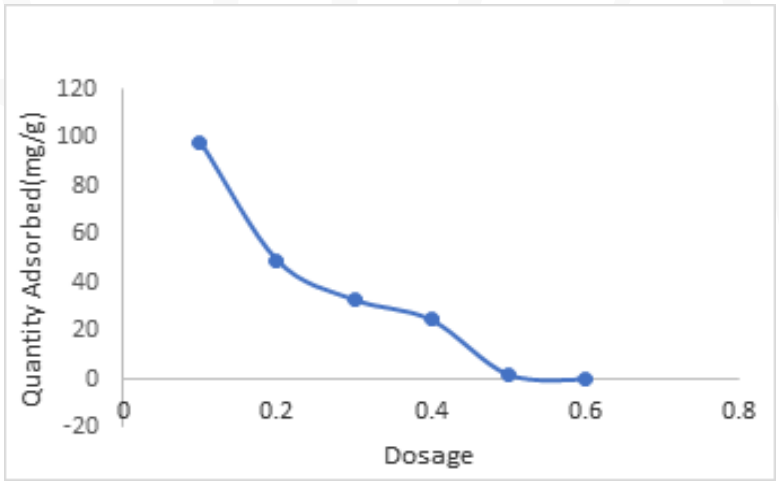

Fig. 3e: Effect of Adsorption Dosage on the adsorption of RhB onto TCFs-Pa [(Agitation speed (150 rpm), contact time (120 mins), temperature (30±01 ºC), adsorbate concentration (10 mg/l)].

3.8 Adsorption Kinetic Studies

The results of adsorption kinetics of RhB onto TCFs-Pa are presented in Table 2. The pseudo-second-order model best fit the kinetic data, indicating chemisorption as the rate-controlling step. Notably, the initial adsorption rate increased with initial adsorbate concentration, suggesting enhanced mass transfer driving forces and increased dye molecule diffusion towards the adsorbent surface. This phenomenon aligns with previous research [12; 22], highlighting the importance of concentration-dependent mass transfer in facilitating rapid adsorption. The pseudo-second-order model's suitability confirms that RhB uptake onto TCFs-Pa is governed by chemisorptive interactions, providing valuable insights into the adsorption mechanism [1].

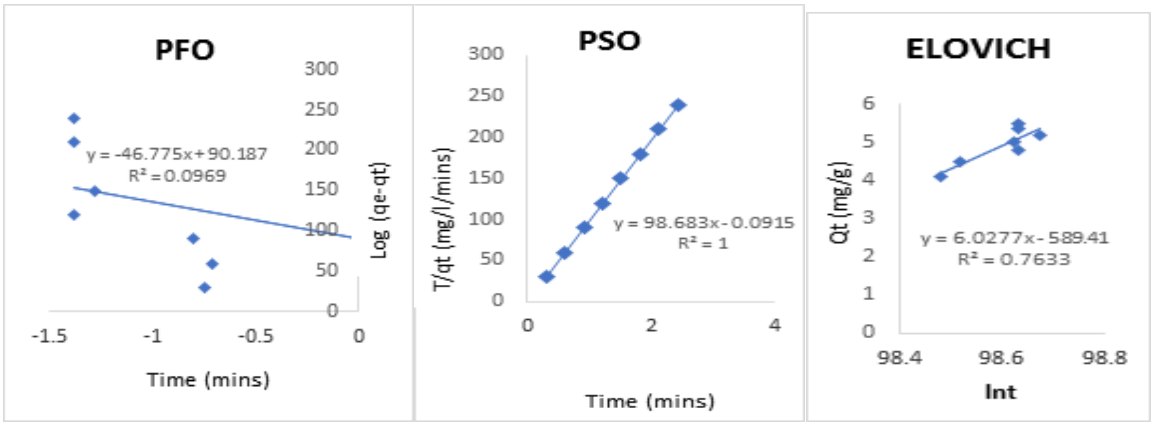

Fig. 4: Kinetic models for adsorption of RhB onto TCFs-PA

Table 2: Kinetic models for adsorption of RhB onto TCFs-PA

Isotherms	Parameters	Values
Pseudo-first order	$K_1(min^{-1})$ Qe, cal (g/g) R^2	-108162 1.0 x E-9216 1
Pseudo-second order	$K_2(min^{-1})$ Qe, cal (g/g) R^2	-4212.3238 0.009938 0.0969
Elovich	α β R^2	0 -109.8901099 0.7633

3.9 Isothermal studies

The adsorption data were analyzed using various isotherm models under controlled conditions of initial RhB concentration (Co) = 100 mg L^{-1}, adsorbent dose (W) = 0.3 g, temperature = 30 °C, contact time = 180 min, and agitation speed = 150 rpm. The adsorption isotherm describes the equilibrium relationship between the amount of substance adsorbed and its concentration in the bulk fluid phase at a constant temperature. This fundamental relationship is essential for distinguishing between different temperature-dependent adsorbents-adsorbates interaction and selecting the most suitable ones for specific applications [6;7]. To accurately describe the experimental data, several isotherm models were examined, including two-parameter models (Freundlich, Langmuir, and Temkin) and three-parameter models (Dubinin-Radushkevitch, D-R). Notably, the Langmuir and Temkin models demonstrated exceptional fit to the adsorption isotherm, with correlation coefficients (R^2) of 0.9994 and 0.9833, respectively. These high R^2 values indicate that the Langmuir and Temkin models accurately describe the adsorption behavior of RhB onto TCFs-Pa, suggesting a homogeneous monolayer adsorption process. The fitted parameters for each model are presented in Table 3, providing a comprehensive understanding of the adsorption mechanism.

Negative Langmuir constant (n): This may indicate poor model fitting or an inappropriate data range. Normally, the Freundlich constant *n* should be greater than 1, indicating favourable adsorption [4].

Extremely high values of Kf (Freundlich) or AT (Temkin): These may result from: Poor fit of the model to the experimental data and Parameter correlation or overfitting.

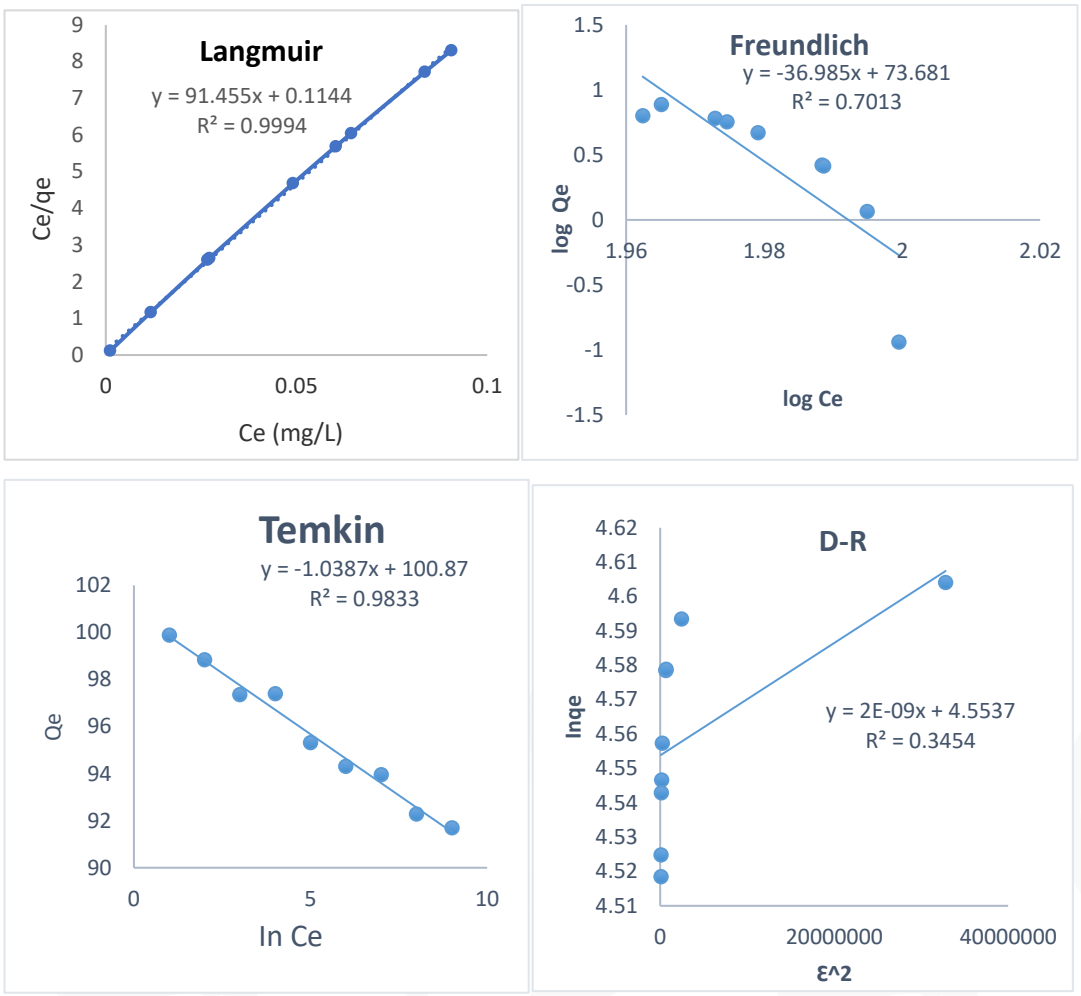

Fig. 5: Adsorption Isotherms for adsorption of RhB onto TCFs-Pa

Table 3: Freundlich, Langmuir, Temkin and D-R Isotherms data

Isotherms	Parameters	Values
Freundlich	n K_f (mol/g) R^2	-0.02704 $4.797x10^{73}$ 0.7013
Langmuir	Q_m (mg/g) K_L (L/mg) R^2	10.93 800.4 0.9994
Temkin	B A_T R^2	-1.0387 $1.35x10^{43}$ 0.9833
D-R	B_D (mol^2kL^{-2}) Qm (mg/g) E (kJ/mol) R^2	$2x10^{-9}$ 95.51 15811 0.3454

The thermodynamic parameters for RhB adsorption onto TCFs-Pa, presented in Table 4, revealed the negative ΔH value confirms the exothermic nature of the process, while the positive ΔS value suggests an increase in disorder or randomness at the solid-solution interface during adsorption. These findings are consistent with previous studies [3;17], validating the thermodynamic results and emphasizing the significance of temperature-dependent adsorption behavior in understanding the adsorption mechanism [27].

A negative enthalpy change ($\Delta H < 0$) indicates an exothermic process, suggesting that the adsorption of RhB onto CFAC is accompanied by the release of heat. A positive Gibbs energy change ($\Delta G > 0$) implies that the adsorption process is non-spontaneous under the given conditions. A positive entropy change ($\Delta S > 0$) indicates an increase in disorder or randomness, potentially due to the displacement of solvent molecules or increased freedom of the adsorbate.

The apparent contradiction between physisorption and chemisorption can be resolved by recognizing that adsorption on CFAC does not occur through a single mechanism. Although the low BET surface area and limited microporosity suggest that physisorption is not the dominant process, weak physical interactions may still contribute to the initial uptake of adsorbate molecules. However, the observed kinetic and isotherm behavior indicates the involvement of stronger interactions, implying a significant contribution from chemisorption. This is likely due to the presence of surface functional groups on CFAC, which promote specific interactions such as electrostatic attraction or π–π interactions. Consequently, the adsorption process is best described as a combined mechanism, in which initial physisorption is followed by chemisorption at active surface sites, thereby resolving the apparent inconsistency between the two interpretations

Furthermore, the Van't Hoff plot, illustrated in Fig. 6, provides additional insight into the thermodynamic properties of the adsorption process.

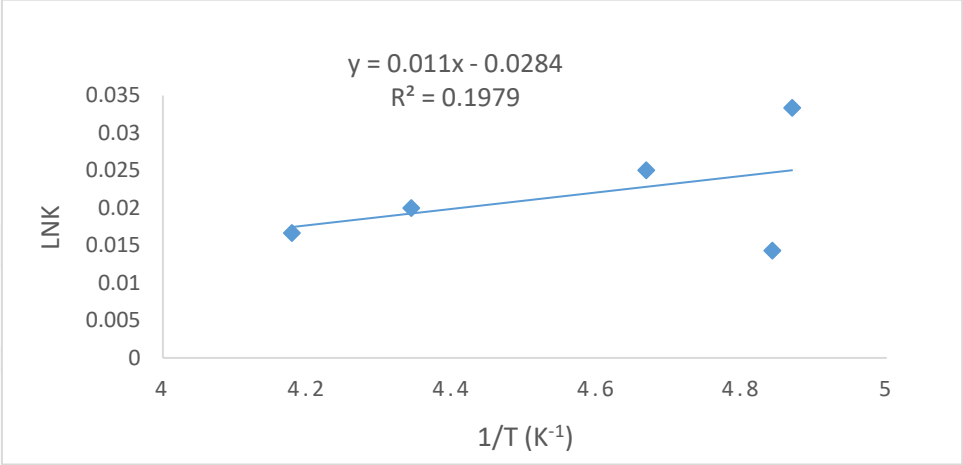

Fig 6: Van't Hoff plot for adsorption of RhB onto TCFs-Pa

Table 4: The thermodynamics parameters (ΔH, ΔS, and ΔG) evaluated from the van't Hoff plot

T (K)	ΔG (KJ/mol)	ΔH (KJ/mol)	ΔS (J/mol/K)
303	0.070	-0.0913	0.236

4.0 Conclusion

This study demonstrates that chicken feather–derived activated carbon (CFAC) is a highly effective adsorbent for the removal of Rhodamine B (RhB) from aqueous solutions. The TCFs-PA was characterized using Fourier transform infrared spectroscopy (FTIR), scanning electron microscopy (SEM), and Brunauer–Emmett–Teller (BET) analysis. BET Analysis was employed to determines surface area & porosity on the adsorbent surface. The adsorbent exhibited a surface area of 48.140 m^2/g, a pore volume of 0.057 cm^3/g, and an average pore size of 2.647 nm.

Physicochemical properties of TCFs-PA CFAC, including bulk density (0.99 g/cm^3), moisture content (0.4%), ash content (3.0%), iodine value (≈ 550 mg/g), and electrical conductivity (0.31 µS/cm), were also determined at pH 7.9 which proved that, it is an alkaline adsorbent and a temperature of 25.9 °C. The observed agreement between the iodine number and BET surface area supports the conclusion that CFAC is characterized by a low proportion of micropores, which may

influence its adsorption performance (minimal shift), C-H stretching C=C stretching and C=C bending (1489.1482.509cm-1).

FTIR analysis was employed to identify the functional groups present on the adsorbent surface. The FTIR spectra of activated carbon samples TCFs-PA the composite, and Rhodamine B–adsorbed carbon is presented in Figures 1. The TCFs-PA spectrum displayed characteristic peaks at 3429.778 - 3275.983 cm^{-1}, the broad peak at 3429.778 - 3275.983 cm^{-1} indicates the presence of free and hydrogen-bonded hydroxyl (–OH) groups on the adsorbent surface, 2938.501-2929.823 cm^{-1}, correspond to conjugated carbonyl (C=O) groups, aromatic C–C bonds, C–N peptide bonds, and S–O interactions, respectively. and 1489.741 -1482.509cm-1, The band Peaks at 1657.035-1651.732 cm^{-1}, further suggests the presence of COO^- and C=C groups, while the peak at 1021.1253 cm^{-1} is associated with amine functional groups and N–H bending vibrations of primary amines ($–NH_2$). The band around 617.30 cm^{-1} represents fingerprint vibrations within the composite structure.

A noticeable reduction in peak intensities after RhB adsorption (Figure 1) confirms effective dye uptake by the composite adsorbent. The active functional groups on the TCFs-PA surface facilitated strong interactions with the dye molecules, thereby enhancing the adsorption process. UV–Vis spectrophotometric analysis showed that RhB exhibited a maximum absorption wavelength (λmax) at 554 nm when scanned between 200 and 1000 nm, and residual dye concentrations were determined at this wavelength. Correlation coefficient R^2 greater than 0.99 shows the linearity of the calibration curve. UV/Visible Spectrophotometry was therefore adopted for the analysis of residual Rhodamine B in subsequent experiments.

The maximum adsorption capacity of TCFs-PA was achieved at a dosage of 0.1 g, with a qe value of 98.28 mg/g, pH 6, temperature 30°C in contact time 180 mins., indicating that CFAC is highly effective even at low adsorbent dosages. CFAC achieved a removal efficiency of 98.48% with an adsorption capacity of the adsorption data fitted well with the Langmuir $R^2 = 0.9994$ and Temkin $R^2 = 0.9833$ isotherm models and followed pseudo-second-order $R^2 = 1$ and elovich kinetics, $R^2 = 0.7633$ confirming monolayer adsorption and chemisorption as the dominant mechanism.

Desorption–adsorption studies using 1.0 M HCl demonstrated good reusability of TCFs-PA, with acceptable performance over three consecutive cycles and an overall capacity loss of approximately 27%. Iodine Number was to determines adsorption capacity (mg/g). This combination of thermodynamic parameters suggests that while the adsorption process releases heat, the overall spontaneity is influenced by the entropy and temperature, as described by the equation $\Delta G = \Delta H - T\Delta S$, where the entropic contribution ($T\Delta S$) may dominate the enthalpic contribution, leading to a positive ΔG.

The adsorption of Rhodamine B (RhB) onto Chemically Functionalized Activated Carbon (CFAC) was investigated, revealing insights into its thermodynamic characteristics. The positive Gibbs energy change ($\Delta G > 0$) indicates the process is non-spontaneous under the studied conditions. A negative enthalpy change ($\Delta H < 0$) suggests the adsorption is exothermic, while a positive entropy change ($\Delta S > 0$) points to increased system randomness, likely due to solvent displacement. These findings imply that CFAC's adsorption of RhB involves heat release but is influenced by entropic factors, as per $\Delta G = \Delta H - T\Delta S$, where the $T\Delta S$ term likely drives the non-spontaneity. This study highlights CFAC's potential for RhB removal, warranting further exploration of operational parameters for enhanced efficacy.

Overall, TCFs-PA derived from poultry waste represents a low-cost, eco-friendly, and sustainable adsorbent for the treatment of dye-contaminated wastewater. This waste to resource approach provides a viable strategy for poultry waste management while addressing water pollution challenges. Future studies should focus on large-scale production, and performance evaluation in real industrial wastewater systems to further validate its practical applicability.

Declaration of generative AI and AI assisted technologies in the writing process

To improve readability and language, the authors used AI tool for editing the content during the preparation of this paper. We hereby declare that we have reviewed and edited the content as required and take full responsibility for the content of the paper.

Reference

1. Abdallah, M., Ahmed, M. and Ahmed, E.A. (2024). Utilization of aquatic biomass as biosorbent for sustainable production of high surface area nano–microporous material for removing two dyes from wastewater. Scientific Reports, Vol. 14, No. 1, pp. 44–71.
2. Abdullahi, M.R. and Nwosu, F.O. (2022). Equilibrium and kinetic studies on the removal of mordant black 11 dye from aqueous solution and real tannery effluents using $CuFe_2O_4$/AC nanocomposites. Applied Journal of Environmental Engineering Science, Vol. 8, No. 4, pp. 1–10.
3. Abdus-Salam, N. and Adekola, F.A. (2006). Comparative dissolution of natural goethite samples in HCl and HNO_3. Journal of Applied Sciences and Environmental Management, Vol. 10, No. 2, pp. 11–17.
4. Adekola, F.A. and Oba, I.A. (2017). Biosorption of formic and acetic acids from aqueous solution using activated carbon from shea butter seed shells. Applied Water Science, Vol. 7, pp. 1775–1784.
5. Ahmed, M.J. (2016). Application of agriculturally based activated carbons by microwave and conventional activations for basic dye adsorption. Journal of Environmental Chemical Engineering, Vol. 4, No. 1, pp. 89–99.
6. Ajiboye, T.O., Oyewo, O.A. and Onwudiwe, D.C. (2021). Adsorption and photocatalytic removal of Rhodamine B from wastewater using carbon-based materials. FlatChem, Vol. 29, Article 100277.
7. Al-Gheethi, A.A., Azhar, Q.M., Kumar, P.S., Yusuf, A.A., Al-Buriahi, A.K., Mohamed, R.M.S.R. and Al-Shaibani, M.M. (2022). Sustainable approaches for removing Rhodamine B dye using agricultural waste adsorbents: A review. Chemosphere, Vol. 287, Article 132080.
8. Al-Ghouti, M.A. and Al-Absi, R.S. (2020). Mechanistic understanding of the adsorption and thermodynamic aspects of cationic methylene blue dye onto cellulosic olive stones biomass from wastewater. Scientific Reports, Vol. 10, Article 15928.
9. Alsawy, T., Rashad, E., El-Qelish, M. and Mohammed, R.H. (2022). A comprehensive review on the chemical regeneration of biochar adsorbent for sustainable wastewater treatment. NPJ Clean Water, Vol. 5, No. 1, Article 29.
10. Chennouf-Abdellatif, Z., Cheknane, B., Zermane, F., Gaigneaux, E.M., Mohammedi, O. and Bouchenafa-Saib, N. (2017). Equilibrium and kinetic studies of methyl orange and Rhodamine B adsorption onto prepared activated carbon based on synthetic and agricultural wastes. Desalination and Water Treatment, Vol. 67, pp. 284–291.
11. Foo, K.Y. and Hameed, B.H. (2010). Insights into the modeling of adsorption isotherm systems. Chemical Engineering Journal, Vol. 156, No. 1, pp. 2–10.
12. Inyinbor, A.A., Adekola, F.A. and Olatunji, G.A. (2016). Kinetics, isotherms and thermodynamic modeling of liquid phase adsorption of Rhodamine B dye onto *Raphia hookeri* fruit epicarp. Water Resources and Industry, Vol. 15, pp. 14–27.
13. Kittappa, S., Jais, F.M., Ramalingam, M., Mohd, N.S. and Ibrahim, S. (2020). Functionalized magnetic mesoporous palm shell activated carbon for enhanced removal of azo dyes. Journal of Environmental Chemical Engineering, Vol. 8, No. 5, Article 104081.
14. Kuśmierek, K., Fronczyk, J. and Świątkowski, A. (2023). Adsorptive removal of Rhodamine B dye from aqueous solutions using mineral materials as low-cost adsorbents. Water, Air, and Soil Pollution, Vol. 234, No. 8, Article 531.
15. Liu, H., Liu, S., Xue, B., Lv, Z., Meng, Z., Yang, X. and He, K. (2018). Ground-level ozone pollution and its health impacts in China. Atmospheric Environment, Vol. 173, pp. 223–230.
16. Liu, Y., Gao, H., Li, Z. and Han, R. (2024). Magnetic bio-composite based on zirconium- and chitosan-modified activated carbon from peanut husk with enhanced antibacterial and adsorptive potential for alizarin red and Congo red in wastewater. International Journal of Biological Macromolecules, Article 132995.

17. Mishra, S., Cheng, L. and Maiti, A. (2021). The utilization of agro-biomass/byproducts for effective bio-removal of dyes from dyeing wastewater: A comprehensive review. Journal of Environmental Chemical Engineering, Vol. 9, No. 1, Article 104901.
18. Moon, W.C. (2019). A review on interesting properties of chicken feather as low-cost adsorbent. International Journal of Integrated Engineering, Vol. 11, No. 2, pp. 1–8.
19. Sathasivam, K.V. and Logesh, K. (2021). Impact of agriculture on economic growth in Nigeria: A co-integration analysis. American Journal of Economics and Finance Research, Vol. 7, No. 2, pp. 68–78.
20. Shirvanimoghaddam, K., Ebrahimi, A. and Yoosefian, M. (2022). Environmental hazard of Rhodamine B in water and wastewater treatment: A comprehensive review. Science of the Total Environment, Vol. 808, Article 151893.
21. Singh, P., Kumar, S. and Kumar, K. (2025). Biogenic synthesis of *Allium cepa*-derived magnetic carbon dots for enhanced photocatalytic degradation of methylene blue and Rhodamine B dyes. Biomass Conversion and Biorefinery, Vol. 15, No. 1, pp. 869–887.
22. Sivalingam, G. and Jayabalakrishnan, R. (2019). Adsorption of methylene blue onto chemically modified *Strychnos potatorum* seed. Journal of Environmental Management, Vol. 231, pp. 1314–1324.
23. Teo, S.H., Ng, C.H., Islam, A., Abdulkareem-Alsultan, G., Joseph, C.G., Janaun, J. and Awual, M.R. (2022). Sustainable toxic dyes removal with advanced materials for clean water production: A comprehensive review. Journal of Cleaner Production, Vol. 332, Article 130039.
24. Tran, M.L. (2024). One-step preparation of activated pomelo peel biochar using H_3PO_4 for removal of methylene blue: Performance, isotherm, and kinetic studies. Biomass Conversion and Biorefinery, pp. 1–13.
25. Wang, L., Shi, C., Pan, L., Zhang, X. and Zou, J.J. (2020). Rational design, synthesis, adsorption principles and applications of metal oxide adsorbents: A review. Nanoscale, Vol. 12, No. 8, pp. 4790–4815.
26. Wang, X. and Wang, Q. (2021). Research on the impact of green finance on the upgrading of China's regional industrial structure from the perspective of sustainable development. Resources Policy, Vol. 74, Article 102436.
27. Yao, L., Zhang, L., Wang, R., Chou, S. and Dong, Z. (2016). A new integrated approach for dye removal from wastewater by polyoxometalates-functionalized membranes. Journal of Hazardous Materials, Vol. 301, pp. 462–470.
28. Zhang, X., Li, Y., Wu, M., Pang, Y., Hao, Z., Hu, M. and Chen, Z. (2021). Enhanced adsorption of tetracycline by iron- and manganese-oxides-loaded biochar: Kinetics, mechanism, and column adsorption. Bioresource Technology, Vol. 320, Article 124264.